

Detection of R- Peaks in Electrocardiogram based on Wavelet Transform and Wavelet Approximation

Imtiyaz Ahmad Wani

Department of Mathematics,
Sandip University, Nashik, Maharashtra, India
Email: wanimtiyaz85@gmail.com

Afroz

Department of Mathematics,
Maulana Azad National Urdu University, Hyderabad, India
Email: afrozjmi123@gmail.com

Rayees Ahmad

Department of Mathematics,
Maulana Azad National Urdu University, Hyderabad, India
Email: darrayees83@gmail.com

Received: 02 April, 2022 / Accepted: 22 July, 2022 / Published online: 29 July 29, 2022

Abstract.: The diseases which are associated with the human heart can be detected through a procedure known as the electrocardiogram that is an electrical activity of the human heart. The clinical analysis of ECG faces problems in its interpretation due to the poor recording environment where unwanted noise is getting contaminated into it in the form of different artifacts viz motion artifacts, loose lead artifact, baseline wandering, muscle tumour artifacts etc. To get noise-free electrocardiogram wavelet theory plays an important role. This paper talks about the framework of approximation of an electrocardiogram signal by wavelet theory. On obtaining the denoised electrocardiogram, prominent peaks and R peaks -part of QRS complex are detected. The proposed algorithm is applied to the ECG recording No. 100m.mat obtained from MIT-BIH database.

AMS (MOS) Subject Classification Codes: 42C40

Key Words: Wavelet, Wavelet Transform, Electrocardiogram, Approximation, R Peak and MATLAB.

1. INTRODUCTION

QRS complex detection is the fundamental necessity in the analysis of the electrocardiogram signal. Because it allows different ways to study other associated characteristic waves in ECG and more importantly knowledge about heart rate variability. Since electrocardiogram is the electrical activity of the human heart. Therefore, it acts as a tool for

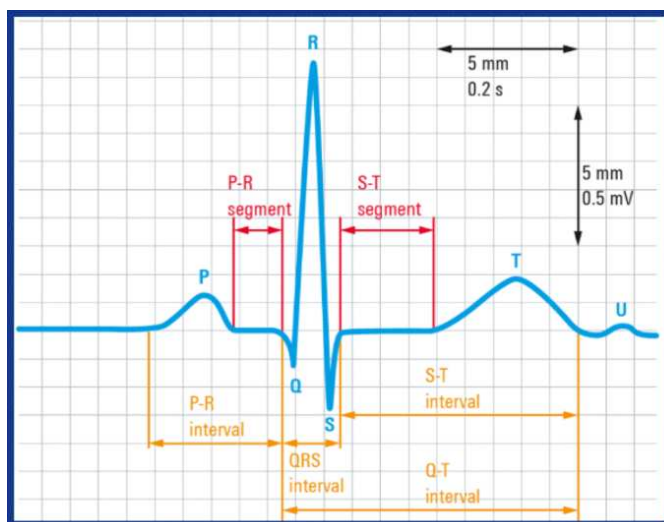


FIGURE 1. One Cardiac Cycle.

cardiovascular system analysis. Moreover, different cardiac pathologies will be diagnosed and discussed under its interpretation process. Thus, it can be said ECG is an act of atrial and ventricular depolarization and repolarization. In this process, P wave and QRS complex exist due to atrial and ventricular depolarization. While, T wave represents ventricular repolarization shown in Figure.1 The figure is adopted from [2].

In this paper, we mainly focus on R-peak which is a part of the QRS complex. The detection of this complex and other aspects related to it like peak detection has clinical importance. This can be done through different ways like the estimation of statistical indicators that in a way evaluate the cardiovascular status of the heart [17],[4]. The foremost imperative portion of ECG is QRS complex and diverse strategies and calculations have been proposed for its investigation and translating ECG [5] [21] [10]. QRS complex originally developed by Pan and Tompkins [12]. The drawback of their algorithm was that the frequency variation in the QRS complex negatively affects their performance. Therefore, Hamilton and Tompkins developed a real-time QRS detection algorithm in the C language [9]. Bandpass filtering and temporal filtering [7] were also applied for QRS complex detection but did not provide a simple way of selecting the bandwidth of the filter and width of the sliding window [19]. Different technologies, computing power, algorithms, methods and other signal processing approaches that help in the detection of QRS complex are available in the literature. All these proposed approaches are in a way based on digital filters and statistical methods. Few among them are Markov Models [4][18], Artificial Neural Networks [18], Mathematical Morphologies [20], Genetic Algorithms [13], Derivative based Algorithms [3][12] and other methods in the literature. The algorithms that are based on wavelet transforms play an important role in denoising an ECG and analyzing it at a different time and frequency resolution scales, so that the QRS complex is distinguished [14].

Therefore, different research works mentioned in the above works convey that wavelet transformation is applied in achieving their respective goals mostly in the form of algorithms. In this paper, we will make use of the approximation of a signal with the help of wavelet theory. The main focus is on the detection of peaks and the prominent peaks in the electrocardiogram. The subject for study is taken from MIT-BIH [8] namely 100m.mat file as shown in Figure. 3. The whole study is targeting the following goals:

- Prominent peaks
- All peaks in the electrocardiogram represented by locs
- Numerical differences that are taken with the preceding locs known as cycles
- Mean of the cycles

The procedure for getting above mentioned goals is based on an algorithm that has a couple of steps that are simulated in MATLAB-2017 and discussed in section 3 (proposed algorithm) of this paper. In section 2 (Methodology), the methods and tools are discussed based on wavelet theory and its approximation procedure.

2. METHODOLOGY

2.1. Continuous Wavelet Transformation. Let $x(t)$ be signal and ψ be a wavelet function then,

$$CWT_x^\psi = \frac{1}{\sqrt{|s|}} \int x(t) \psi^* \left(\frac{t-\tau}{s} \right) \quad (2.1)$$

Here the transformed signal is a function of two variables τ and s , known as translation and scale parameter and ψ is called a wavelet function.

2.2. Wavelet function. Wavelet means a little wave. Littleness implies this wave has limited length and wave nature implies it is oscillatory in nature. Mathematically, in [8] wavelet function is defined as,

$$\psi_{s,\tau}(t) = \frac{1}{\sqrt{|s|}} \psi \left(\frac{t-\tau}{s} \right) \quad (2.2)$$

Where, $\psi \in L^2(\mathbb{R})$ and this set is an orthonormal wavelet basis in the function space $L^2(\mathbb{R})$. The parameter τ is utilized to analyze the signal over time axis and the scale parameter 's' gives possibility of local analysis of the signal.

Mathematically in [14], CWT of signal $x(t)$ and the basis function $\psi_{\tau,s}$ is defined as i.e.

$$CWT_x^\psi = \langle x(t), \psi^*(\tau, s) \rangle = \int x(t) \psi^*(\tau, s)(t) \quad (2.3)$$

Here for every (τ, s) , (3) gives wavelet coefficient as outcome among them some are large and some are small in magnitude for more details refer to [11].

2.3. Discrete wavelet transformation. In [1] [6] Discrete Wavelet Transform is defined as:

$$f(t) = \sum_{m,n=-\infty}^{\infty} \langle f(t), \psi_{m,n}(t) \rangle \quad (2.4)$$

Here in [1] scaling 's' and translation parameter τ are discretized by introducing two constants a_0 and b_0 such that $a_0 = 2$ and $b_0 = 1$ are used so that it gives binary dilation 2^{-m} and dyadic translation .

The very first hallmarks of wavelet transformation are scaling and wavelet functions. In this paper, we understand this framework with the help of an important wavelet function that has an explicit form, known as Haar wavelet.

This is the simplest wavelet in explicit form and is defined as,

$$\psi(x) = \begin{cases} 1 & : 0 \leq x < \frac{1}{2} \\ -1 & : \frac{1}{2} \leq x < 1 \\ 0 & : otherwise \end{cases} \quad (2.5)$$

The corresponding scaling function of this Haar Wavelet is,

$$\phi(x) = \begin{cases} 1 & : 0 \leq x < 1 \\ 0 & : otherwise \end{cases} \quad (2.6)$$

This wavelet has a compact support. Let ϕ be a scaling function (Haar Scaling function) then the function of the form $\phi(t - k) : k \in Z$ is its translations over the time axis. Such a series of functions are orthonormal i.e

$$\int_{-\infty}^{\infty} \phi(t - m)\phi(t - n) = \begin{cases} 1 & : m = n \\ 0 & : m \neq n \end{cases} \quad (2.7)$$

The set of above translations of ϕ forms a space denoted by V_0 defined as,

$$V_0 = span(\bar{\phi}(2^0 t - k)) \quad (2.8)$$

Any signal or function $f(t)$ in V_0 can be formed as,

$$f(t) = \sum_{k=-\infty}^{\infty} a_k \phi(t - k) \quad (2.9)$$

Where, a_k are scalar coefficients.

Here V_0 can be rewritten as $V_0 = span(\bar{\phi}(2^0 t - k))$ that means V_0 is a space formed by $\phi(t)$ having scale factor equal to $2^0 = 1$. Similarly,

$$V_1 = span(\bar{\phi}(2^1 t - k)) \quad (2.10)$$

is a functional space spanned by $\phi(2^1 t - k)$ with scaling factor equal to 2^1 . Generally, the space V_j is spanned by the set of functions $\phi(2^j t - k) : j \in Z$ having scalar factor equal to $2^j = 1$.

Thus any function $f(t)$ can be formed in V_j as,

$$f(t) = \sum_{k=-\infty}^{\infty} a_k \phi(2^j t - k) \quad (2.11)$$

Keeping the scaling function $\phi(t)$ as Haar scaling function in the above construction, we will easily verify that

$$...V_{-2} \subset V_{-1} \subset V_0 \subset V_1 \subset V_2 \subset V_3...$$

Such a sequence is known as nested spaces formed by the scaling function.

A question occurs here, what is missing in V_{j-1} that makes V_{j-1} a subset of V_j . The

answer lies in the spaces formed by another important function associated with scaling function known as wavelet function.

Let $\psi(t)$ be a wavelet function then the set $\psi(t - k) : k \in Z$ is called its translations and we can easily verify that this series is orthonormal i.e.

$$\int_{-\infty}^{\infty} \psi(t - m)\psi(t - n) = \begin{cases} 1 & m = n \\ 0 & m \neq n \end{cases} \quad (2. 12)$$

The span of $\psi(t - k)$ gives us a space denoted by W_0 defined as,

$$W_0 = span(\psi(t - k)) = span(\psi(2^0t - k)) \quad (2. 13)$$

Similarly,

$$W_1 = span(\psi(2^1t - k)) \quad (2. 14)$$

That is a space with a scale parameter 2^1 . More generally, space with scale parameter equal to 2^1 is defined as,

$$W_j = span(\psi(2^jt - k)) \quad (2. 15)$$

Thus any function $f(t)$ can be constructed with the help of basis function $\psi(2^jt - k)$ in the space W_j as:

$$f(t) = \sum_{k=-\infty}^{\infty} b_k \psi(2^jt - k) \quad (2. 16)$$

Here b_k are the scalars. Keeping in view the definition of $\psi(t)$ (Haar Wavelet function), we can easily verify that,

$$...W_{-2} \subset W_{-1} \subset W_0 \subset W_1 \subset W_2 \subset W_3...$$

Now if we combine the spaces V_j and W_j [14], we can conclude that:

$$V_j = V_{j-1} \oplus W_{j-1} \quad (2. 17)$$

The sum \oplus is the orthogonal sum and it also conveys that the combination of the basis of V_{j-1} and W_{j-1} represents a signal in the next higher or finer space V_{j-1} .

This construction leads us towards an important analysis known as Multi-resolution Analysis. Its central theme is to decompose a signal or a function into approximations and details in the form of zoom in and zoom out. Increasing resolution leads us to zoom in and decreasing resolution leads us to zoom out. Such a procedure helps us in going arbitrary close to the original signal. This is done by a well-known procedure called projection of a signal $f(t)$ over the spaces defined above.

Let $f_j(t) \in V_j$ with a scaling factor $\frac{1}{2^j}$. Suppose the basis function for spanning is $2^{\frac{j}{2}}\phi(2^jt - k)$ that is orthonormal with normalizing factor $2^{\frac{j}{2}}$, then the projection of $f(t)$ over V_j is defined as,

$$f_j(t) = \sum_{k=-\infty}^{\infty} \alpha_{j,k} 2^{\frac{j}{2}} \phi(2^jt - k) \quad (2. 18)$$

where,

$$\alpha_{j,k}(t) = \int_{-\infty}^{\infty} f_j(t) 2^{\frac{j}{2}} \phi(2^jt - k) dt$$

$$g_j(t) = \sum_{k=-\infty}^{\infty} \beta_{j,k} 2^{\frac{j}{2}} \psi(2^j t - k) \quad (2.19)$$

$$\beta_{j,k}(t) = \int_{-\infty}^{\infty} g_j(t) 2^{\frac{j}{2}} \psi(2^j t - k) dt$$

Illustration:

Find the approximation of $f(x)$ defined as,

$$f(x) = \begin{cases} x + 1 : & 0 \leq x \leq 3 \\ 0 : & \text{otherwise} \end{cases} \quad (2.20)$$

Sol. For $j=0$, define $f_0(x) \in V_0$ then the scale is equal to $\frac{1}{2^j} = \frac{1}{2^0} = 1$, that shows a window of length equal to 1.

Therefore, the basis function for the Haar Scaling function is

$$2^{\frac{j}{2}} \phi(2^j x - t) = 2^{\frac{0}{2}} \phi(2^0 x - t) = \phi(x - t), k \in Z$$

Therefore from equation (18), we get,

$$f_0(x) = \sum_{k=0}^2 \alpha_{j,k} 2^{\frac{j}{2}} \phi(2^j x - k) = \sum_{k=0}^2 \alpha_{j,k} \phi(x - k) \quad (2.21)$$

Now,

$$\alpha_{0,0} = \int_{-\infty}^{\infty} f_0(x) 2^{\frac{j}{2}} \phi(2^j x - k) dx = \int_{-\infty}^{\infty} f_0(x) \phi(x) dx = \int_0^1 (x - 1) dx = \frac{3}{2}$$

Again,

$$\alpha_{0,1} = \int_1^2 (x + 1) 2^1 \phi(x - 1) dx = \int_1^2 (x + 1) \cdot 2 \cdot 1 \cdot dx = 5$$

Similarly,

$$\alpha_{0,2} = \int_2^3 (x + 1) \cdot 2 \cdot 1 \cdot dx = 7$$

Thus, $f_0(x) = \frac{3}{2} \phi(x) + 5 \phi(x - 1) + 7 \phi(x - 2)$.it is the projection of $f(x)$ over the space V_0 . Now steps for finding the projection $f(x)$ over the space W_0 with the help of wavelet function ψ defined above. For $j=0$, we get scale equal to $2^{\frac{0}{2}} = 1$ and approximation $g_0(x)$ defined as in (19)

$$g_0(x) = \sum_{k=0}^2 \beta_{0,k} \psi(x - k) \quad (2.22)$$

Here,

$$\beta_{0,0} = \int_{-\infty}^{\infty} g_0(x) \psi(x) dx = \int_0^1 (x + 1) \psi(x) dx = -\frac{1}{4}$$

$$\beta_{0,1} = \int_1^2 (x + 1) \psi(x - 1) dx = -\frac{1}{2}$$

$$\beta_{0,2} = \int_2^3 (x + 1) \psi(x - 2) dx = -\frac{25}{4}$$



FIGURE 2. Flowchart and Program for Peak Detection

Therefore,

$$g_0(x) = \frac{-1}{4}\psi(x) - \frac{1}{2}\psi(x - 1) - \frac{25}{4}\psi(x - 2)$$

This way we have approximated $f(x)$ into two spaces V_0 and W_0

On changing the scale, we can similarly approximate the signal $f(x)$ over the nested space V_1 and W_1 then in general over the space V_j and W_j . Here one should note that more is the scaling value the more accurately we approximate the given signal $f(x)$. Again as $V_j = V_{j-1} \oplus W_{j-1}$, it means if we have projections of a signal in V_{j-1} , W_{j-1} , and add them orthogonally we lead to space V_j . That means we are moving up the ladder. This is how mathematically a signal is approximated at different levels of scaling.

2.4. Flowchart for Algorithm. The flow chart for the whole analysis is shown in figure 2 with program for peak detection on its right side:

The first five steps in the algorithm [1] shown in the flow chart are given below:

2.5. Algorithm. This algorithm is proposed by the author in his research paper as mentioned in self-citation[1]. The steps are:

- (1) A noisy ECG signal is first decomposed with the help of the wavelet transform at 3rd level into approximation and detail coefficients.
- (2) Obtained a threshold value of detailed coefficients at each stage with the help of a formula, $T = \sigma \sqrt{\log(N)}$
- (3) After third step, apply the wavelet packet transformation for its denoising at the threshold value obtained in step 2.
- (4) Denoise the ECG signal recieved and then reconstructed it by using inverse wavelet packet transformation from MATLAB wavelet toolbox.

But here different wavelet functions are used in the process for denoising the signal with added noise shown in Figure 4. Once reconstruction is done we will obtain a denoised

signal called synthesized ECG signal shown in Figure 5. Now apply the program shown above in order to achieve the required results for the last two steps of the algorithm in MATLAB- 2017.

3. RESULTS AND DISCUSSION

The program is first executed for original signal 100m.mat and results are shown in Table 1 as a list of locs for the original signal 100m.mat and in Table 2 as a list of cycles which is a difference of locs. The locs represents sample value across ECG Signal as the possible highest peaks. The second part of this program gives us prominent peaks and the average of cycles is taken as shown in Table 3. The same program is then executed for those entire denoised signals which are obtained after denoising an added noisy signal 100m.mat with the help of different wavelet functions and using wavelet packet transformation. All the outcomes are shown in Table 4 and Table 5. Also for the sake of sample the locs are shown in Figure 6.

Similar list of locs and corresponding cycles can be obtained and shown for the denoised signal when using different wavelet function in the algorithm and denoised signal in the program but due to huge list of values, we will just demonstrate the proposed algorithm and the program for evaluation and is then shown in the list of tables as mentioned in above paragraph. Following are the key outcomes of the proposed algorithm:

- (1) The maximum number of prominent peaks that coincide with the original signal listed in Table 2, we can call them as R-Peaks are found in db6 wavelet function when used in the algorithm for denoising and obtain Prominent peaks. Also, the mean of cycles is 8.578 that is near to the original mean found in Table 1
- (2) In the Haar wavelet, no peak is found when applied in the proposed algorithm. The reason may be because of its discontinuity or level of decomposition or possibly threshold value.
- (3) In Daubechies series, the number of maximum peaks obtained is in the following decreasing order db6, db5, db3, db8, db7, db4, db9, and db10. But in terms of the mean of cycles, the variation from the original mean is very high in all of them except db5 and then db6.
- (4) In the series of Coiflet wavelet maximum number of correct R-peaks is found in coif-5 followed by coif-4, coif-2, coif-1, and coif-3 in its decreasing order. Again the mean of cycles is also very near in coif-5 but other wavelets in the series gives very poor results.
- (5) Similarly in the symlet series, it is sym-7 that gives the maximum number of correct R-peaks. The other wavelets in the series detect the correct number of R-peaks in the order of sym-8, sym-6, sym-5, sym-4, and sym-2. In terms of the mean of cycles sym-7 again gives better value than other wavelets in the series.

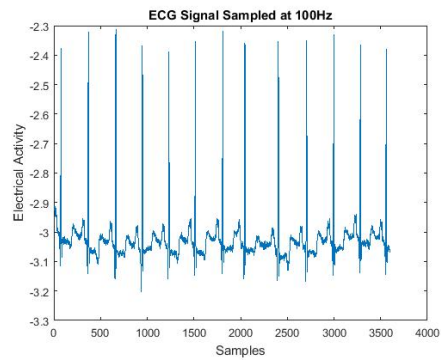


FIGURE 3. Original ECG Signal 100m.mat without noise obtained from MIT-BIH database

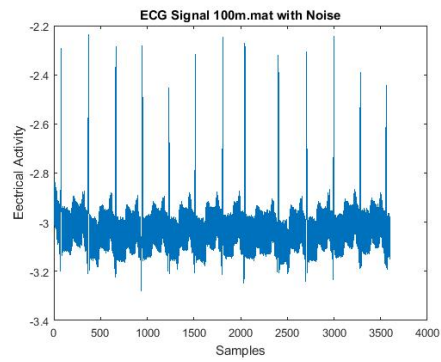


FIGURE 4. ECG Signal 100m.mat added with Noise

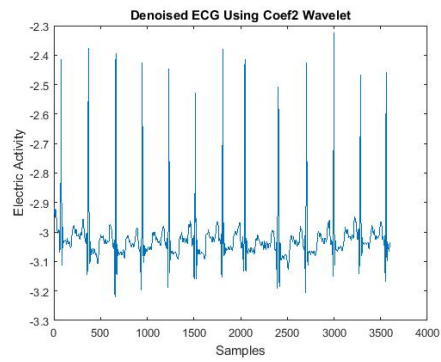


FIGURE 5. Synthesised Signal (Denoised) Using Coif2 Wavelet Function

TABLE 1. List of locs (sample value) after applying the Program on 100m.mat

9	14	20	26	31	39	46	55	57	78	88	94
98	101	104	111	116	134	141	143	145	154	166	172
177	196	207	212	215	225	231	137	242	244	248	259
267	272	283	285	291	299	309	313	323	332	334	341
343	346	351	355	371	385	394	400	404	415	417	424
435	442	447	452	455	459	464	471	479	485	489	502
505	512	514	519	524	529	531	538	548	561	573	579
583	585	592	604	607	609	617	626	632	645	664	674
676	679	681	689	700	710	713	716	724	735	739	754
756	772	789	799	801	813	821	825	827	830	832	836
838	850	859	861	866	879	885	890	894	899	909	927
948	962	969	974	981	994	999	1010	1014	1016	1027	1034
1036	1040	1047	1053	1058	1064	1070	1077	1083	1087	1091	1093
1101	1105	1112	1120	1124	1160	1166	1168	1172	1176	1178	1182
1190	1196	1207	1209	1214	1232	1250	1255	1261	1268	1278	1280
1299	1310	1316	1319	1321	1324	1328	1335	1352	1359	1362	1364
1369	1381	1384	1389	1394	1396	1406	1413	1442	1449	1452	1454
1466	1480	1488	1491	1495	1516	1526	1531	1562	1567	1569	1575
1681	1683	1693	1701	1706	1708	1711	1732	1747	1754	1760	1770
1778	1784	1810	1827	1839	1844	1866	1869	1880	1888	1892	1899
1905	1909	1916	1933	1940	1952	1958	1981	1986	1999	2006	2017
2020	2024	2026	2028	2046	2055	2058	2060	2065	2077	2079	2082
2090	2094	2096	2103	2109	2114	2120	2122	2126	2136	2138	2144
2150	2163	2177	2182	2185	2192	2199	2203	2216	2219	2222	2229
2233	2235	2240	2253	2259	2269	2272	2282	2284	2286	2289	2294
2299	2307	2311	2318	2320	2322	2330	2332	2348	2355	2371	2379
2391	2404	2425	2437	2440	2443	2450	2454	2456	2462	2491	2497
2503	2506	2509	2511	2529	2535	2539	2544	2558	2563	2576	2588
2595	2599	2616	2618	2632	2634	2638	2643	2648	2652	2665	2672
2678	2684	2690	2707	2721	2732	2734	2738	2743	2748	2751	2757
2760	2768	2773	2775	2785	2792	2799	2810	2822	2829	2834	2838
2840	2850	2853	2857	2859	2864	2869	2882	2906	2910	2912	2918
2935	2938	2947	2952	2972	2983	2999	3008	3019	3021	3035	3038
3044	3051	3056	3058	3062	3066	3068	3073	3075	3080	3087	3117
3122	3135	3141	3151	3154	3157	3159	3164	3169	3171	3175	3188
3195	3205	3207	3212	3214	3224	3236	3249	3266	3284	3296	3308
3312	3315	3318	3320	3322	3326	3331	3338	3349	3357	3362	3364
3368	3373	3375	3381	3392	3410	3415	3426	3428	3430	3432	3434
3445	3450	3457	3459	3466	3468	3471	3476	3481	3483	3506	3525
3536	3540	3561	3572	3577	3584	3590					

TABLE 2. R Peaks (Prominent peaks) and Mean of cycles (Mean of cycles represents average of differences of locs) for 100m.mat

Prominant Peaks(R-Peaks)	78 371 664 948 1232 1516 1810 2046 2404 2707 2999 3284 3561
Mean (Cycles)	5.5386

TABLE 3. R- Peak of Denoised ECG 100m.mat at Decomposition Level 3 by applying above mentioned program using different wavelet functions listed in the table

Wavelet Functions	Prominent peaks (R-Peaks)												
Haar	No Peak Found												
db2	82	370	375	666	1946	1234	1514	1810	2042	2050	2402	2706	3002
db3	78	371	664	947	1232	1516	1811	2044	2403	2707	2999	3283	3562
db4	79	369	664	945	1232	1513	1808	2047	2401	2704	2999	3281	3560
db5	77	372	665	948	1232	1516	1811	2045	2404	2707	2999	3283	3561
db6	78	371	664	948	1232	1516	1810	2045	2404	2707	2999	3284	3560
db7	76	371	663	948	1233	1516	1811	2044	2403	2707	2997	3283	3562
db8	79	370	663	948	1232	1517	1808	2046	2404	2705	2999	3284	3559
db9	76	371	665	947	1233	1515	1810	2044	2403	2707	2997	3283	3562
db10	78	372	663	949	1231	1517	NA	2046	2405	2707	2998	3285	3559
Coif1	75	371	659	667	1235	1515	1811	2043	2403	2707	2995	3283	3563
Coif2	79	371	664	947	1231	1516	1811	2047	NA	2707	2999	3283	3559
Coif3	NA	NA	NA	948	NA	1517	1811	NA	NA	NA	NA	NA	NA
Coif4	78	371	664	947	1231	1516	1811	2046	2404	2707	2999	3283	3560
Coif5	78	371	664	948	1232	1517	1811	2045	2404	2707	2999	3283	3561
Sym2	78	370	666	946	1234	1518	1810	2402	2602	2706	3000	3285	3562
Sym3	76	372	660	948	1229	1516	1812	2044	2404	2708	2996	3284	3574
Sym4	77	371	663	947	1231	1517	1811	2045	2404	2707	2999	3283	3560
Sym5	76	371	666	947	1234	1515	1810	2043	2403	2707	3001	3283	3583
Sym6	77	372	664	949	1232	1517	1811	2045	2405	2706	2999	3284	3561
Sym7	77	371	664	948	1232	1516	1811	2045	2404	2706	2999	3283	3561
Sym8	79	371	665	947	1232	1516	1811	2046	2404	2707	2999	3283	3560

TABLE 4. Mean of cycles by using different wavelet functions

Wavelets	Haar	db2	db3	db4	db5	db6	db7	db8	db9	db10	Coif1
Mean (Cycles)	24.738	12.46	23.729	17.039	6.725	8.578	21.183	21.42	21.239	22.734	16.18
Wavelets	Coif2	Coif3	Coif4	Coif5	Sym2	Sym3	Sym4	Sym5	Sym6	Sym7	Sym8
Mean (Cycles)	20.80	24.0	12.47	6.373	12.081	14.274	9.24	20.422	11.08	6.697	13.434

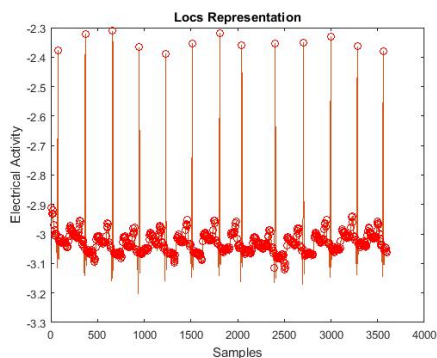


FIGURE 6. Locs Representation(Represents peaks in 100m.mat as a whole whether smaller one or highest one)

TABLE 5. Number of Correct and False R- Peaks in relationship with Table 1

Wavelets	Haar	db2	db3	db4	db5	db6	db7	db8	db9	db10	Coif1
No. of Correct R Peaks	NA	1	7	3	7	11	4	6	2	2	2
No. of False R Peaks	NA	12	6	10	6	2	9	7	11	11	11
Wavelets	Coif2	Coif3	Coif4	Coif5	Sym2	Sym3	Sym4	Sym5	Sym6	Sym7	Sym8
No. of Correct R Peaks	4	1	8	9	2	4	4	3	5	8	7
No. of False R Peaks	9	12	5	4	11	9	9	10	8	5	5

3.1. Conclusion. This paper talks about the application of wavelet theory in signal processing in the context of approximation by applying wavelet packet analysis. Under this application, we have targeted the electrocardiogram signal in which peaks are detected. The program is developed that detects the peaks available in the denoised signal and list of prominent peaks are listed in Table 3 and mean of cycles are listed in Table 4. The concluding points for the whole study is that due to the difference of some properties in wavelet functions, variations of results are noticed in the analysis.

In simple words, the analysis shows that db-6 gives better outcomes then coif-5 followed by symlet-7. But as concluding remark, the analysis has scope of modification for getting less error in obtaining R Peak values(samples) very near to the original one.

REFERENCES

- [1] Afroz and W. A. Imtiyaz, *Denoising of Electrocardiogram Based on Norm Parameter using Wavelet Packet Transform*, Int. J. Eng. Adv. Technol, **09**, No. 1 (2019) 3377-3383.
- [2] A. D. Algarni, N. F. Soliman, H. A. Abdallah, et al. *Encryption of ECG signals for telemedicine applications*, Multimed Tools Appl. **80**(2021) 10679-10703 . <https://doi.org/10.1007/s11042-020-09369-5>
- [3] M. L. Ahlstrom and W. J. Tompkins, *Automated high-speed analysis of Holter tapes with microcomputers*, IEEE Transactions on Biomedical Engineering, **10**(1983), 651-657.
- [4] M. Altuve, G. Carrault, A. Beuchee, P. Pladys and A. I. Hernandez, *On-line apnea-bradycardia detection using hidden semi-Markov models*, Annual International Conference of the IEEE Engineering in Medicine and Biology Society, (2011) 4374-4377

- [5] S. A. Chouakri, F. Berekci-Reguig and A. Taleb-Ahmed, *QRS complex detection based on multi wavelet packet decomposition*, Applied Mathematics and Computation, **217**, No.23(2011) 9508-9525.
- [6] L. Debnath and F.A. Shah, *Wavelet transforms and their applications*, Boston: Birkhauser. (2002)
- [7] H. A. N. Dinh and D. K. Kumar, N. D. Pah, and P. Burton, *Wavelet for QRS detection*, proceeding of the 23rd annual EMBS international conference, Turkey, **2**(2001)1883-1887.
- [8] Al. Goldberger, Lan Amaral, L. Glass, JM. Hausdorff, PCh. Ivanovh, RG. Mark, JE. Mietus, GB. Moody, C-K. Peng and HE Stanley, *MIT-BIH Arrhythmia Database* updated 7 June 2018, <https://archive.physionet.org/physiobank/database/mitdb/>
- [9] P.S. Hamilton and W. J. Tompkins, *Quantitative investigation of QRS detection rules using the MIT/BIH arrhythmia database*, IEEE transactions on biomedical engineering, **33**, No.12 (1986) 1157-1165.
- [10] S. Kadambe, R. Murray and G. F. Boudreaux-Bartels, *Wavelet transform-based QRS complex detector*, IEEE Transactions on biomedical Engineering, **46**, No. 7(1999) 838-848.
- [11] R. T. Ogden, *Essential Wavelets for Statistical Applications and Data Analysis*. 1997.
- [12] J. Pan, and W. J. Tompkins, *A real-time QRS detection algorithm*, IEEE transactions on biomedical engineering, **3**(1985) 230-236.
- [13] R. Poli, S. Cagnoni and G. Valli, *Genetic design of optimum linear and nonlinear QRS detectors*, IEEE Transactions on Biomedical Engineering, **42**, No.11(1995) 1137-1141.
- [14] K. D. Priya, G. S. Rao and P. S. Rao, *Comparative analysis of wavelet thresholding techniques with wavelet-wiener filter on ECG signal*, Procedia Computer Science, **87**(2016) 178-183.
- [15] S. Savalia, E. Acosta and V. Emamian, *Classification of cardiovascular disease using feature extraction and artificial neural networks*, Journal of Biosciences and Medicines, **5**, No. 11(2017) 64-79.
- [16] K. P. Soman, N. G. Resmi and K. I. Ramachandran, *Insight Into Wavelets: From Theory to Practice*, American Journal of Respiratory and Critical Care Medicine. (2010).
- [17] L. Sornmo, and P. Laguna, *Bioelectrical signal processing in cardiac and neurological applications*, Academic press, **8** (2005)
- [18] S. Sotelo, W. Arenas and M. Altuve, *QRS complex detection based on continuous density hidden Markov models using univariate observations*. In Journal of Physics: Conference Series, **1002**, No. 1 (2018) 012009.
- [19] N. V. Thakor, J. G. Webster and W. J. Tompkins, *Estimation of QRS complex power spectra for design of a QRS filter*, IEEE Transactions on biomedical engineering, **11**(1984) 702-706.
- [20] S. Yazdani and J. M. Vesin, *Adaptive mathematical morphology for QRS fiducial points detection in the ECG*. In Computing in Cardiology, IEEE, (2014)725-728 .
- [21] C. Zeng, H. Lin, Q. Jiang and M. Xu, *QRS Complex Detection Using Combination of Mexican-hat Wavelet and Complex Morlet Wavelet*. J. Comput., **8**, No. 11(2013)2951-2958.